5. J. C. Claoué-Long, Z. Zichao, M. Guogan, D. Shaohua, *Earth Planet. Sci. Lett.* **105**, 182 (1991).
6. P. R. Renne and A. R. Basu, *Science* **253**, 176 (1991).
7. G. B. Dalrymple *et al.*, *Eos* **72**, 570 (1991).
8. A. Baksi and E. Farrar, *ibid.*, p. 570.
9. G. A. Izett, G. B. Dalrymple, L. W. Snee, *Science* **252**, 1539 (1991).
10. J. L. Wooden *et al.*, *Eos* **72**, 571 (1991).
11. V. A. Fedorenko, *Sov. Geol. Geophys.* **22**, 66 (1981).
12. J. C. Claoué-Long, W. Compston, M. Fanning, J. Roberts, *Chem. Geol.*, in press.
13. The assumption of concordance can be tested by comparison of the mean to the mode and by recalculation of the mean after omission of all high-U grains. The mean is not significantly different from the mode, nor is it changed if high-U grains are omitted, which justifies the assumption of concordance.
14. L. P. Zonenshain, M. I. Kuzmin, L. M. Natapov, Eds., *Geology of the USSR: A Plate-tectonic Synthesis*, vol. 21 of *Geodynamics Series* (American Geophysical Union, Washington, DC, 1990); G. F. Makarenko, *Int. Geol. Rev.* **19**, 1089 (1977).
15. A. N. Khramav and V. P. Rodionov, in *Global Reconstructions and the Geomagnetic Field During Palaeozoic*, M. W. McElhinny, Ed. (Kluwer Academic, Dordrecht, the Netherlands, 1981), vol. 10, pp. 99–115; E. Irving and L. G. Parry, *Geophys. J. R. Astron. Soc.* **7**, 395 (1963); J. G. Ogg and M. B. Steiner, *Earth Planet. Sci. Lett.* **107**, 69 (1991).
16. M. Haag and F. Heller, *Earth Planet. Sci. Lett.* **107**, 42 (1991).
17. V. V. Zolotukhin and A. I. Al'Mukhamedov, in *Continental Flood Basalts*, J. D. Macdougall, Ed. (Kluwer Academic, Dordrecht, the Netherlands, 1988), pp. 273–310.
18. D. M. Raup and J. J. Sepkoski, Jr., *Science* **231**, 833 (1986).
19. W. T. Holser and M. Magaritz, *Mod. Geol.* **11**, 155 (1987); W. T. Holser *et al.*, *Nature* **337**, 39 (1989).
20. J. B. Pollack, O. B. Toon, E. F. Danielsen, D. J. Hofman, J. M. Rosen, *Geophys. Res. Lett.* **10**, 989 (1983); D. J. Hofmann and J. M. Rosen, *J. Geophys. Res.* **92**, 9825 (1987); M. R. Rampino and S. Self, *Nature* **310**, 677 (1984); S. Self and M. R. Rampino, *Eos* **69**, 83 (1988).
21. H. Sigurdsson, in "Global Catastrophes in Earth History: An Interdisciplinary Conference on Impacts, Volcanism, and Mass Mortality," V. L. Sharpton and P. D. Ward, Eds. *Geol., Soc. Am. Spec. Pap. 247* (1990), pp. 99–110.
22. W. T. Holser and M. Margaritz, *Geochim. Cosmochim. Acta* **66**, 3297 (1992).
23. We thank D. Devir and J. Bitmead for their assistance in preparing the manuscript.

1 May 1992; accepted 23 September 1992

Manipulation of the Reconstruction of the Au(111) Surface with the STM

Y. Hasegawa and Ph. Avouris*

Modification of the reconstruction of an Au(111) surface with a scanning tunneling microscope (STM) is demonstrated. This modification is accomplished by transferring a number of surface atoms to the STM tip to generate a surface multivacancy (hole), which modifies the stress distribution at the surface. The structural changes that follow the tip-induced surface perturbation are imaged in a time-resolved manner. The structural modification is the result of both short-range interactions, which lead to local atomic relaxation, and long-range elastic interactions, which produce large-scale rearrangements.

In recent years, the STM (*1*) has emerged as a unique tool for the atomic and nanometer-scale modification and manipulation of materials (*2*, *3*). In particular, experimental approaches have been developed that allow the reversible transfer of atoms between the sample and the STM tip by means of chemical tip-sample interactions and voltage pulses (*4*, *5*). Here, we demonstrate the manipulation of the reconstruction of the Au(111) surface. This reconstruction involves an array of surface dislocations whose pattern we are able to modify with the STM. To accomplish this, we induce "local" perturbations by transferring a number of surface atoms to the tip (*4*). The resulting vacancy modifies the stress distribution at the surface, and through substrate-mediated long-range elastic interactions it leads to large-scale atomic rearrangements. We are able to follow these atomic relaxation processes in a time-resolved manner, and we find evidence not only of single atom motion (diffusion) but also of concerted motion of large numbers of atoms. An important implication of this work is that, because of the elastic coupling between surface atoms, there are limits, which are material-dependent, to how small and how local STM-induced modifications can be.

A variety of diffraction techniques (*6*–*8*) and the STM (*9*–*11*) have been used to study the reconstruction of the Au(111) surface, which has a $22 \times \sqrt{3}$ structure (that is, a structure with a unit cell whose sides are, respectively, 22 and $\sqrt{3}$ times the nearest neighbor Au atom distance in the unreconstructed surface). This surface structure is considered to be the result of a balance between two opposing tendencies (*12*): the surface layer would like to contract in order to compensate for its reduced coordination, whereas opposing this contraction the underlying substrate potential favors a commensurate surface layer. The misfit between the surface layer and the substrate leads to the formation of a periodic array of pairs of partial dislocations (domain walls), which separate alternating domains in which surface atoms occupy face-centered-cubic (fcc) and hexagonal close-packed (hcp) sites (Fig. 1). The surface atoms at the dislocation lines occupy bridge instead of hollow sites, and in STM images of the surface (Figs. 2 and 3) the dislocation lines appear as ridges with a height of ~0.1 to 0.2 Å. The unit cell of this reconstruction (22 times the unit length) contains 23 surface atoms instead of 22, thus allowing a 4.4% contraction along the $\langle 1\bar{1}0 \rangle$ direction in the surface layer. Because of the small energy difference between fcc and hcp sites, the widths of fcc and hcp domains are different; the wider domain is presumed to have the fcc structure, which is energetically more favored. Although the $22 \times \sqrt{3}$ reconstruction relieves the stress along the $\langle 1\bar{1}0 \rangle$ direction, stress remains in other directions.

To relieve the stress in a more uniform manner, a surface superstructure is formed consisting of a regular alternation of uniaxial domains arranged in a zigzag pattern. This rotational domain superstructure, usually referred to as a herringbone structure, is energetically favored because of the substrate-mediated elastic interactions between the rotational domain boundaries (*13*, *14*). Because the reduction of surface stress is the main driving force for this reconstruction, the surface structure is expected to be sensitive to perturbations that affect the stress distribution at the surface.

From a study of large numbers of STM images, we find that there is a strong tendency for the dislocation lines to be perpendicular to the surface steps. Steps are free edges of the surface layer, and therefore the stress component perpendicular to the steps must be zero. Because surface stress is still present along the dislocation lines, these lines tend to align themselves perpendicular to the steps so as to relieve the surface stress. This observation suggested that, if step-like structures can be made artificially on the surface, the pattern of dislocation lines could be modified intentionally and the structural changes that take place could be imaged with the STM. For example, an STM-generated hole (multivacancy) on the surface is surrounded by steps and thus should be able to relieve the surface stress around it.

In this work, we applied voltage pulses between the STM tip and the sample to remove surface atoms, generate holes at specific surface locations, and thus modify the surface reconstruction (pattern of dis-

IBM Research Division, T. J. Watson Research Center, Yorktown Heights, NY 10598.

*To whom correspondence should be addressed.

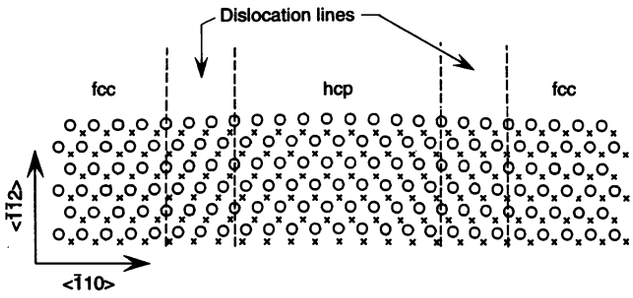

Fig. 1. In-plane structure of the Au(111) surface with a $22 \times \sqrt{3}$ reconstruction. The circles and crosses correspond to atoms in the first and second surface layers, respectively. Surface atoms in both sides of the figure lie on fcc sites, whereas atoms in the center of the figure lie on hcp sites. The domain walls (dislocation lines) involve atoms in bridge sites.

location lines). The method of making a hole on the surface is the same as that reported before (*4*): We remove atoms from the surface by first bringing the tip close to the sample to establish an interaction between tip and sample, and then we apply a voltage pulse. The barrier for atom transfer between the tip and sample is reduced at close distances, and the high electric field generated by the voltage pulse further reduces the barrier, induces directionality, and makes the transfer of the Au atoms possible. By this "chemically assisted field evaporation" (CAFE) mechanism (*4*), we can make holes at specific locations and, if desired, we can redeposit the removed atoms at other locations. We can control the size of a hole by adjusting the pulse height, pulse width, and the distance between the tip and sample.

All experiments reported here were done under ultrahigh vacuum conditions with a base pressure of $\sim 1 \times 10^{-10}$ torr. The Au samples used in this study were prepared in situ by evaporation of Au on cleaved mica at room temperature and subsequent annealing at ~900 K for about 1 min. The samples prepared in this way have large (111) facet planes with the same reconstruction (*15, 16*) as that observed on a single crystal Au(111) sample. All STM images shown in this report were taken with the use of a tungsten tip with a sample bias voltage of +0.5 to +1.0 V and a tunneling current of 100 pA. Under these conditions, no changes in the dislocation patterns were observed, except in the case of intentional manipulation.

Several STM images of an Au(111) surface were taken in a time sequence (Fig. 2). The area of the surface shown in the images is about 200 by 200 Å. Figure 2A is an STM image taken before a hole was made: pairs of partial dislocation lines (their separation is about 44 Å) are seen with a periodicity of 63 Å; that is, 22 times the lattice spacing of the Au(111) surface. At the top and bottom of the picture are two rotational domain boundaries where the dislocation lines bend by 120°. (We use the term "kink" to describe these bending regions.) Figure 2B shows a hole that we generated (~10 Å in diameter) on top of a dislocation line, using the CAFE technique (pulse height: +1.5 V, pulse width: 10 ms). STM line-scans show the depth of the hole to be equal to a monoatomic step height, which indicates that only surface atoms have been removed. Subsequent to the creation of the hole by the STM tip, we followed the changes induced in the surface structure by recording STM images as a function of time (Fig. 2, B through F).

After the generation of the hole (Fig. 2B), the two segments of the dislocation line on which the hole was formed change their relative positions slightly: the upper segment of the dislocation line shifts to the right, while the lower segment shifts to the left. This change is due to stress relief by the hole. Judging from the direction of the shifts, we find that the tension of the dislocation lines, which tends to make them straight, is a driving force of these shifts. However, the effect of the hole is not only local. The adjacent dislocation line was also deformed around its bending point (kink), leading to the generation of a protrusion (*17*) (see upper left part of the image). The induced protrusion is far away from the hole, ~80 Å, as compared to the size of hole (~10 Å). This deformation of dislocation lines provides a direct verification of the proposed long-range elastic interactions at this surface and will be discussed in more detail below.

The next image (Fig. 2C) shows that the original two dislocation lines have split. The dislocation lines in the upper half have been joined to form a U-shaped loop, while the lower portion has been pinned at the hole. The protrusion generated at the elbow position after the hole was made has also disappeared in Fig. 2C. As time progresses, the size of the hole decreases as diffusing Au atoms enter the hole (*18*). The shape of the hole also changes, and faceting is observed. The two dislocation segments are orientated perpendicular to the facets. The squashed appearance of the U-shaped loop in Fig. 2C suggests that a repulsive interaction between the hole and the U-shaped loop

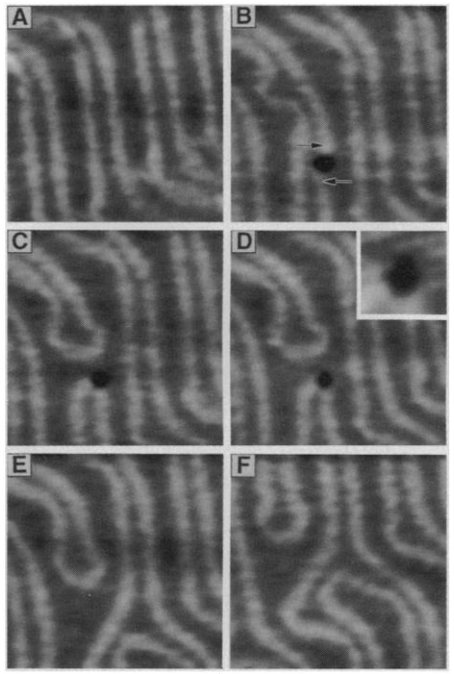

Fig. 2. STM images of the Au(111) surface (200 by 200 Å) obtained: (**A**) before making a hole, (**B**) after the hole was formed, (**C**) 0 to 6 min after (B), (**D**) after 6 to 12 min, (**E**) after 12 to 18 min, and (**F**) after 50 min.

may be present. In Fig. 2D, the hole is now very clearly faceted (inset) with steps perpendicular to the $\langle \bar{1}\bar{1}2 \rangle$ direction. Atoms at $\langle \bar{1}\bar{1}2 \rangle$ steps have a high coordination number (sevenfold coordination), and therefore $\langle \bar{1}\bar{1}2 \rangle$ steps are expected to be most stable.

Finally, in Fig. 2E, we observe that, within 6 min after Fig. 2D, the hole has disappeared and a new arrangement of the dislocation lines has emerged. This arrangement involves the two lower branches of the dislocation lines, previously stabilized by the hole, fusing with the neighboring dislocation pair to their right to give a characteristic forked structure. This forked structure is quite stable, as can be seen in the image (Fig. 2F) taken 1 hour later. Without the hole, the U-shaped loop is seen to attain a more symmetric structure. The most interesting observation involves the abruptness with which the hole disappeared, simultaneously with the change of the dislocation pattern.

In another experiment (not shown here) we observed that a similarly made hole was not eliminated but changed its relative position during the change of the dislocation pattern. To make a dislocation line, $1/\sqrt{3}$ additional atoms are required per unit length in the $\langle \bar{1}\bar{1}2 \rangle$ direction. Thus, the change of dislocation pattern requires diffusion or rearrangement of surface atoms, and this explains the long time scale over which the modification takes

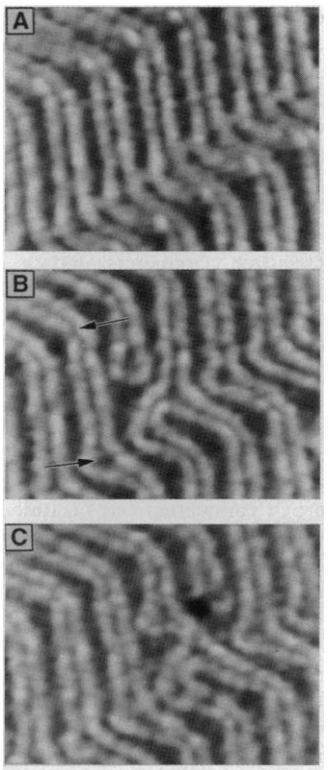

Fig. 3. STM images of the Au(111) surface (500 by 380 Å): (**A**) and (**B**) were taken before and after making the hole shown in Fig. 2, respectively; (**C**) was taken after making another hole in (B).

place. Most important, the STM results show that, on this surface, structural changes occur not only by single atom motion but also by the concerted motion of large numbers of atoms through the motion of dislocation patterns.

Figures 3A and 3B are larger area STM images (500 Å by 380 Å) obtained before and after the manipulation shown in Fig. 2. Before a hole was made (Fig. 3A), the Au(111) surface had the familiar structure of dislocation lines. After a hole was made, the dislocation lines were rearranged to form a forked structure (Fig. 3B). We can continue manipulating the surface structure by generating new holes and changing the stress distribution. As an example, Fig. 3C shows an STM image obtained after another hole was made at the neck of the forked structure. In this image, the pair of dislocation lines on which the hole was made is split, making a new U-shaped dislocation loop. The other split side is switched back to the left and is connected to the U-shaped loop produced by the previous manipulation.

These results show that one can modify and manipulate the pattern of dislocation lines of the Au(111) surface by locally removing surface atoms with the STM tip. The STM experiments provide evidence for two kinds of interactions that lead to the surface modification: local effects and long-range effects. Local effects involve relaxations similar to those taking place at steps; the hole deforms the dislocation lines by relieving the surface stress around them. As a result of these local effects, dislocation lines terminated by a hole are forced to bend so as to be perpendicular to the edge of the hole (see Fig. 2, C and D). However, the effect of holes is not restricted to only their immediate vicinity because dislocation lines far from a hole are also deformed (Figs. 2 and 3). By these long-range effects, kink sites (that is, dislocation lines at rotational domain boundaries) are most affected. This finding suggests that the observed deformations are the result of elastic interactions between domain boundaries, which may be responsible for the herringbone structure on the surface (*14*). Elastic long-range forces applied at domain boundaries are determined by the stress distribution on the surface, and a hole made on the surface perturbs this distribution. In the manipulation shown in Fig. 2, the hole was placed almost midway between two kink sites located in the upper part and lower part of the images, respectively. However, only the kink site in the upper part of the images was affected by the hole. As can best be seen in Fig. 3B (see arrows), the two kink sites have different structures. At the upper kink site the narrow hcp domain pinches off, whereas at the lower kink site it bulges (*11*). Our experiments suggest that kink sites of the type in the upper part of the image are more easily deformed by the generation of a hole.

The response of the Au surface to the perturbation induced by a hole is site-dependent, apparently reflecting the difference in the local stress distribution. Figure 4 shows schematically some of our observations involving kink sites of the type in which the hcp region is "pinched off." An intermediate structure (not shown in Fig. 2) composed of a closed loop is shown in structure d. We observe this structure around kink sites only early (that is, within the first 2 to 3 min) after the creation of the hole. This loop has three protrusions pointing in the $\langle \bar{1}\bar{1}2 \rangle$ directions and serves as a precursor for the formation of the other structures. Structure A in Fig. 4 shows a protrusion similar to that in Fig. 2. This structure can be generated from the loop pattern in structure d when two of the three protrusions are connected with two U-shaped dislocation loops. Structure B in Fig. 4 can be generated from structure d when only one protrusion is connected with a U-shaped loop. Finally, to form structure C, one protrusion of the loop is extended downward and is inserted between a dislocation pair.

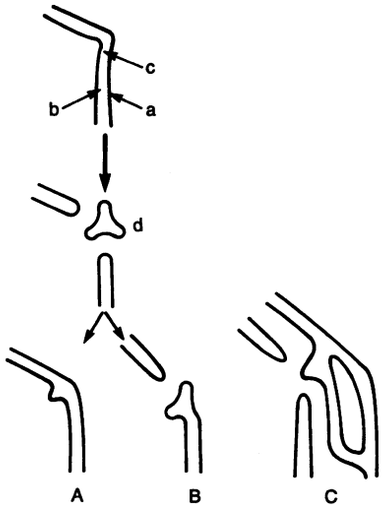

Fig. 4. Typical modified patterns of dislocation lines. Structures A, B, and C are patterns generated by creating a hole at sites a, b, and c, respectively; d is a closed loop structure formed as an initial stage of the modification.

REFERENCES AND NOTES

1. G. Binnig, H. Rohrer, Ch. Gerber, E. Weibel, *Phys. Rev. Lett.* **49**, 57 (1982).
2. C. F. Quate, in *Highlights in Condensed Matter Physics and Future Prospects*, L. Esaki, Ed. (Plenum, New York, 1991), pp. 573–630.
3. J. A. Stroscio and D. M. Eigler, *Science* **254**, 1319 (1991).
4. I.-W. Lyo and Ph. Avouris, *ibid.* **253**, 173 (1991); Ph. Avouris and I.-W. Lyo, *Appl. Surf. Sci.* **60/61**, 426 (1992).
5. D. M. Eigler *et al.*, *Nature* **352**, 600 (1991).
6. J. Perdereau, J. P. Biberian, G. E. Rhead, *J. Phys. F* **4**, 1978 (1974).
7. Y. Tanishiro *et al.*, *Surf. Sci.* **111**, 395 (1981).
8. U. Harten, A. M. Lahee, J. P. Toennies, Ch. Wöll, *Phys. Rev. Lett.* **54**, 2619 (1985).
9. Ch. Wöll, S. Chiang, R. J. Wilson, P. H. Lippel, *Phys. Rev. B* **39**, 7988 (1989).
10. J. V. Barth, H. Brune, G. Ertl, R. J. Behm, *Phys. Rev.* **42**, 9307 (1990).
11. D. D. Chambliss, R. J. Wilson, S. Chiang, *Phys. Rev. Lett.* **66**, 1721 (1991); *J. Vac. Sci. Technol. B* **9**, 933 (1991).
12. M. El-Batanouny, S. Burdick, K. M. Martini, P. Stancioff, *Phys. Rev. Lett.* **58**, 2762 (1987).
13. O. L. Alerhand *et al.*, *ibid.* **61**, 1973 (1988).
14. S. Narasimhan and D. Vanderbilt, *ibid.* **69**, 1564 (1992).
15. V. M. Hallmark *et al.*, *ibid.* **59**, 2879 (1987).
16. M. M. Dovak, C. A. Lang, J. Nogami, C. F. Quate, *Phys. Rev. B* **40**, 11973 (1989).
17. As discussed by Chambliss *et al.* (*11*), there are two kinds of kinks, depending on the Burgers vectors of the dislocation segments that are joined. If the Burgers vectors are not equal, there must be a surface edge dislocation at the kink sites, resulting in a "pointed" structure. The kink site at which the protrusion was formed had an edge dislocation and, by the formation of the protrusion, two additional edge dislocations were created. Their creation requires additional atoms and involves atomic diffusion or vacancy formation.
18. R. C. Jaklevic and L. Elie, *Phys. Rev. Lett.* **60**, 120 (1988).

19. We thank J. E. Demuth and R. Walkup for a careful reading of the manuscript.

12 August 1992; accepted 23 October 1992